Modeling and Simulation of a Bio-Inspired Nanorobotic Drug Delivery System

Qingying Zhao[1] and Lin Lin[2(✉)]

[1] Changshu Institute of Technology, Suzhou, China
qyzhao@cslg.edu.cn
[2] Tongji University, Shanghai, China
fxlinlin@tongji.edu.cn

Abstract. Current targeted drug delivery systems like passive targeting or active targeting are still inefficient because they mainly depend on blood circulation and extravasation. It is significant that drug delivery carriers are capable of autonomously swimming towards target site (e.g., diseased cells or tumors) and releasing drugs. In recent years, targeted drug delivery depending on autonomous swimmers such as nanorobot has been actively studied and a number of solutions have been proposed. In the paper, we propose a nanorobot-based system comprising of nanorobot behavior planning algorithm, drug reception model and adjusting method of release rate for a simulation of local targeted drug delivery. In this system, nanorobots can move and accumulate at target site by simulating bacterial chemotaxis, and determine the timing of drug release relying on quorum sensing. In addition, nanorobots can dynamically adjust the rate of drug release depending on the concentration of tumor biomarker. A simulation environment is established in order to evaluate the nanorobotic drug delivery system. The simulation results show that the nanorobotic drug delivery system can not only deliver drugs effectively at desired location but also enhance efficiency of drug utilization.

Keywords: Molecular communication · Nanorobotic · Targeted drug delivery

1 Introduction

During the past few decades, controlled drug delivery (CDD) has experienced an enormous upswing and brought a series of highly effective pharmaceutical preparations with low toxicity side effects and good compliance. The evolution of the controlled drug delivery mainly includes three stages from its origins to the present. The first stage was the "macro era" of zero-order "controlled" drug

Supported in part by the National Natural Science Foundation of China under Grant 61971314, in part by the Changshu Institute of Technology Scientific Research Fund under Grant KYZ2019003Q.

Y. Chen et al. (Eds.): BICT 2023, LNICST 512, pp. 64–76, 2023.
https://doi.org/10.1007/978-3-031-43135-7_7

delivery devices. Some CDD devices were designed in macroscopic scale in the early days. For example, the Ocusert designed by Alza Corp. was an ophthalmic insert that released the anti-glaucoma drug at a constant rate in the eye, and the Norplant developed by Population Council, Wyeth is a contraceptive subcutaneous implant comprised of six silicone rubber tubes filled with a contraceptive steroid, levo-Norgestrel which can be released at a constant rate [1]. The second stage is the "micro era" of sustained release, biodegradable microparticle delivery systems. Sustain-controlled release system could improve efficiency of drug utilization and plasma concentration by means of injectable, biodegradable drug-loaded microparticles. The third stage is the "nano era" of targeted drug delivery systems.

For the "nano era" of targeted drug delivery, PEGylation, the EPR effect and passive targeting, active targeting with antibodies, peptides and small molecule, cell-specific ligands are the three key technologies stimulating the development of drug nanocarriers as practical clinical realities. PEGylation is referred to as modifying the surface of nanoparticles (drug nanocarriers) with poly (ethylene glycol) [2]. The circulation time and stability of nanoparticles can be enhanced by the PEGylation in circulatory system [3]. The term "EPR" is abbreviation of enhanced permeation and retention first proposed by Professor Hiroshi Maeda [4,5]. Passive targeting is the process of extravasation drug accumulation in diseased tissues such tumors with leaky vasculature, which is commonly known as the enhanced permeation and retention (EPR) effect [6]. Although the longer systemic circulation time achieved by PEGylation [7] contribute to the EPR effect of drug nanocarriers, only a small percent ($< 10\%$) of administered drug nanocarriers actually reach diseased tissues or tumors [8,9]. If ligands are added to the surface of drug nanocarriers, the passive targeting can be improved through the interactions between drug nanocarriers and target receptors. Unfortunately, the specific interactions usually called active targeting [10,11] can occur only when drug nanocarriers and target receptors are in close proximity [2].

It is significant that drug delivery systems are capable of autonomously swimming towards disease site. Autonomous nanoswimmers or systems have been proposed to transport drug molecules in targeted drug delivery. The evolving nanoswimmers can be divided into biological such as modified bacteria, even sperms and synthetic such as nanorobots or nanomachines [12]. Bacteria have been used to carry therapeutic nanoparticles and diagnostic agent to disease site depending on the property of penetrating tissue, target tumors [13–15]. Nanorobots being able to perform tasks at nano-level could be used to travel through human blood vessels and microvasculature. For example, a chemical communication algorithm was proposed by Cavalcanti et al. to coordinate nanorobots to reach tumor site [16]. In addition, nanorobots carrying drugs can be directly injected into the target site of a patient body. After entering into the disease site, nanorobots would release drug molecules to treat disease cells. Since the drug molecules are usually expensive or where lost molecules may cause undesired side effects such as drug overuse or multi-drug resistance [17,18], the timing and rate of drug release become important issues.

Quorum sensing (QS) is a well-known cell-cell communication mechanism in bacteria [19–21]. Bacteria can use quorum sensing to coordinate timing of specific actions. Bacteria start quorum sensing behavior when the concentration of a specific molecules released by them in extracellular environment achieves a specific threshold. For example, when the bioluminescent marine bacterium Vibrio fischeri was alone, that is when they were in dilute suspension, they made no light [22]. When bacteria aggregated to grow to a certain cell number, all the bacteria turned on light simultaneously. Why they can do it is that they can talk to each other with a chemical language called autoinducer (AI). The autoinducers are acylated homoserine lactones (AHL) that regulate positively the lux operon in Vibrio fischeri. The lux can control bioluminescence and upregulate the expression of the AHL-synthase LuxI which produces the AI molecule. LuxR's dimerized complex with AHL can lead to transcriptional activation of LuxI. The concentration of the AHL is dependent not only on its production, but also on the permeability from outside the cell. Namely, the switch of QS is dependent on the AHL concentration just outside the cell. Since the AHL concentration outside is proportional to the number of bacteria, bacteria start quorum sensing when the bacteria density reaches a specific threshold.

This paper proposes a nanorobot-based drug delivery system comprising of Nanorobot Behavior Planning (NBP) algorithm, drug reception model and adjusting method of release rate in order to deliver drugs effectively at local of human body. In the system, nanorobots can accumulate at the target location and determine the timing of drug release relying on quorum sensing. In addition, the NBP algorithm can dynamically adjust the rate of drug release based on the concentration of tumor biomarker.

The rest of the paper is organized as follows. Section 2 presents the NBP algorithm based on bacterial chemotaxis and quorum sensing. The quorum sensing threshold is estimated in Sect. 3. Section 4 presents drug reception model and adjustable drug release based on the concentration of tumor biomarker. In Sect. 5, simulations are conducted and the obtained results are analyzed. Finally, in Sect. 6, the paper is conducted with a summary of results.

2 NBP Algorithm Based on Bacterial Chemotaxis and Quorum Sensing

In this section, the Nanorobot Behavior Planning (NBP) algorithm based on bacterial chemotaxis and quorum sensing is proposed. Firstly, nanorobots make chemotactic movement and determine whether to reach the tumor target site according to the concentration of tumor-related biomarker. Secondly, nanorobots release autoinducers (AI) when reaching tumor target site. When the concentration of AI reaches a specific threshold, nanorobots start release drug molecules. Finally, it is assumed that the concentration of tumor-related biomarker is proportional to the number of tumor cells. Nanorobots adjust drug release rate based on the biomarker concentration.

Table 1. Notations used in NBP algorithm.

Symbol	Description
i	Index of nanorobots
j	Index of motion steps (time)
C	Unit motion size
θ	Nanorobot location
φ	Nanorobot motion direction
T_t	Threshold of tumor biomarker concentration
J	Concentration of tumor biomarker
Q_A	Constant release rate of AI
τ	AI concentration
T_{AIh}	High-threshold of AI concentration
T_{AIl}	Low threshold of AI concentration (Quorum sensing threshold)
Q_D	Adjustable release rate of drug molecules

We formulate the NBP algorithm using the notations shown in Table 1. In the algorithm, each nanorobot is considered as a bacterium with specified chemotaxis and quorum sensing behavior. Let $i \in N$ represent each nanorobot. Let j be the index of time step of nanorobots. Let $\theta^i(j)$ be the location of the ith nanorobot at the jth motion step. Let $J(i,j)$ denote the concentration of tumor biomarker at the location $\theta^i(j)$ of the ith nanorobot. Let $C(i) > 0$ denote a basic motion size that we will use to define the step length during the ith nanorobot moves. Let $\varphi(j)$ denote a unit length random motion direction after a unit motion step. In particular, we let

$$\theta^i(j+1) = \theta^i(j) + C(i)\varphi(j) \tag{1}$$

represent a new position after a motion step of a nanorobot. Let T_t denote a specific threshold of tumor-related biomarker, and

$$J(i,j) \geq T_t \tag{2}$$

indicate that a nanorobot has reached the tumor target site. If a nanorobot detects tumor biomarker and its concentration is less than T_t, the nanorobot will move to a new position of higher concentration. That is, if $J(i,j)$ at position $\theta^i(j)$ is larger than that at $\theta^i(j-1)$, a motion step of size $C(i)$ in the same direction $\varphi(j-1)$ will be taken. Otherwise, the nanorobot moves a step with a random new direction $\varphi(j)$. If a nanorobot detects the concentration of tumor biomarker that meets to Eq. (2), it indicates that the nanorobot has reached the tumor target site. The nanorobot will release AI with a constant rate Q_A and detect the concentration of AI. Let $\tau(i,j)$ denote the concentration of AI at position $\theta^i(j)$ of the ith nanorobot. If the concentration of AI is larger than the high-threshold T_{AIh}, it indicates that population of nanorobots in tumor target site is too many, and the nanorobot will move away from the tumor target site. That is, if $J(i,j)$ at position $\theta^i(j)$ is less than that at position $\theta^i(j-1)$, a motion

Algorithm 1: NBP Algorithm

Input: $i,\ j,\ J(i,j),\ \tau(i,j),\ T_t,\ T_{AIh},\ T_{AIl}$
Output: Nanorobot behavior, Drug release rate Q_D

```
for i=1:N do
    if J(i,j) < T_t && J(i,j) > J(i,j-1) then
        θ^i(j+1) = θ^i(j) + C(i)φ(j-1) ;        // Move a step at the same
        direction
    end
    if J(i,j) < T_t && J(i,j) ≤ J(i,j-1) then
        θ^i(j+1) = θ^i(j) + C(i)φ(j) ; // Move a step at a random direction
    end
    if J(i,j) ≥ T_t && τ(i,j) > T_AIh then
        if J(i,j) ≤ J(i,j-1) then
            θ^i(j+1) = θ^i(j) + C(i)φ(j-1);
        end
        if J(i,j) > J(i,j-1) then
            θ^i(j+1) = θ^i(j) + C(i)φ(j);
        end
    end
    if J(i,j) ≥ T_t && τ(i,j) ≤ T_AIh then
        Δτ(i,j) = Q_A;
    end
    if J(i,j) ≥ T_t && T_AIl ≤ τ(i,j) ≤ T_AIh then
        Drug release rate = Q_D;
    end
end
```

step of size $C(i)$ in the same direction $\varphi(j-1)$ will be taken. Otherwise, the nanorobot will move a step following Eq. (1) with a random new direction. If the concentration of AI is less than the high-threshold T_{AIh}, the nanorobot at position $\theta^i(j)$ will release $\Delta\tau(i,j)$ doses of AI. $\Delta\tau(i,j)$ is an increment of AI, which can be expressed as Eq. (3).

$$\Delta\tau(i,j) = \begin{cases} Q_A, & \tau(i,j) \le T_{AIh}, J(i,j) \ge T_t \\ 0, & \text{otherwise.} \end{cases} \tag{3}$$

The update of AI concentration is shown as Eq.(4).

$$\frac{\partial \tau}{\partial t} = D_A \nabla^2 \tau, \tag{4}$$

where D_A is diffusion coefficient of AI, ∇^2 Laplacian for the dimension considered. If the concentration of AI $\tau(i,j)$ is less than T_{AIh} and larger than the threshold T_{AIl}, the nanorobot will release drug molecules with rate Q_D based on the concentration of tumor-related biomarker. The pseudo code of the algorithm is described as Algorithm 1.

In the algorithm, the calculation of quorum sensing threshold T_{AIl} and the design of adjustable release rate Q_D are described at length in Sect. 3 and Sect. 4 respectively.

3 Calculation of Quorum Sensing Threshold

After AI molecules were released by nanorobots, the concentration of AI reaches a peak in an instant. AI molecules diffuse in the direction of low concentration as time goes on [23]. According to Fick's laws of diffusion, if a nanorobot releases Q AI molecules at time instant $t = 0$, the molecular concentration at any point in space is given by [24]:

$$c(r,t) = \frac{Q}{(4\pi D_A t)^{3/2}} \exp\left(\frac{-r^2}{4D_A t}\right), \tag{5}$$

where D_A is the diffusion coefficient of the AI molecules, t is time and r the distance from the nanorobot location. For AI continuous emission (i.e., releasing a train of bursts of size Q spaced by a period Δt) of single nanorobot, the molecular concentration at any point in space can be derived:

$$\begin{aligned} c_c(r,t) &\approx \frac{1}{\Delta t}\int_0^t c(r,\tau)d\tau \\ &= \int_0^t \frac{Q}{(4\pi D\tau)^{3/2}} \exp\left(-\frac{r^2}{4D\tau}\right)d\tau \\ &= \frac{Q}{\Delta t 4\pi D_A r} erfc\frac{r}{(4D_A t)^{\frac{1}{2}}}. \end{aligned} \tag{6}$$

When time t is large enough, we can obtain

$$c_c(r,t) \approx \frac{Q}{\Delta t 4\pi D_A r}. \tag{7}$$

When Δt is unit time (i.e., Δt =1), Eq.(7) becomes

$$c_c(r,t) \approx \frac{Q}{4\pi D_A r}. \tag{8}$$

For AI continuous emission of multi-nanorobot, we can apply the superposition principle (i.e., the addition of two received emissions will yield the same concentration than the reception of the addition of two emissions) to calculate AI molecular concentration at any point in space because the AI concentration is relatively low and in an scenario devoid of external forces (i.e., free diffusion) [24,25]. It is assumed that N nanorobots are distributed randomly in three-dimensional spherical space and form a cluster. Each nanorobot i locating at $\boldsymbol{p}_i$ releases AI molecules with a constant rate (Q molecules per unit time) and the concentration of AI molecules is low enough. It is assumed that each

nanorobot i is at a distance $d_i = |\boldsymbol{p} - \boldsymbol{p}_i|$ of the evaluated point p. From Eq.(8), we can obtain AI concentration at $\boldsymbol{p}$

$$c_{multi}(\boldsymbol{p}) = \sum_{i=1}^{N} \frac{Q}{4\pi D d_i} = \frac{Q}{4\pi D} \sum_{i=1}^{N} \frac{1}{|\boldsymbol{p} - \boldsymbol{p}_i|}. \tag{9}$$

To simplify solving Eq.(9), we learn from the method in [26]. It is assumed that the nanorobots are arranged in a perfect tridimensional grid so that nanorobot positions are deterministic and symmetric with respect to the center origin $O(0, 0, 0)$. Therefore, the AI concentration at origin $O(0, 0, 0)$ can be calculated from Eq.(9):

$$c_{multi}(\boldsymbol{O}) = \frac{Q}{4\pi D} \sum_{i=1}^{N} \frac{1}{|\boldsymbol{p}_i|}, \tag{10}$$

and the AI concentration at a distance $r > 0$ from origin is

$$c_{multi}(\boldsymbol{p}_r) = \frac{Q}{4\pi D} \sum_{i=1}^{N} \frac{1}{|\boldsymbol{p}_r - \boldsymbol{p}_i|}. \tag{11}$$

Due to the distribution of perfect tridimensional grid, it can be concluded $c_{multi}(\boldsymbol{O}) > c_{multi}(\boldsymbol{p}_r)$, that is, the AI concentration decreases as the distance increases from origin $O(0, 0, 0)$. In addition, it has been demonstrated that the AI concentration of any evaluated point calculated from random distribution of nanorobots approaches the one of perfect tridimensional grid [26]. Hence, in order to ensure an activation of all nanorobots in quorum sensing, it is necessary that the quorum sensing threshold

$$T_{AIl} \geq c_{multi}(\boldsymbol{p}_R) = \frac{Q}{4\pi D} \sum_{i=1}^{N} \frac{1}{|\boldsymbol{p}_R - \boldsymbol{p}_i|}, \tag{12}$$

where the point $\boldsymbol{p}_R$ locates at the edge of the three-dimensional spherical space, i.e., R is the radius of the three-dimensional spherical space.

4 Drug Reception Model and Adjustable Release Rate

Many enzyme inhibitor drugs (EID), such as competitive inhibitor drugs, are noncovalent, reversible inhibitors [27]. Being similar to the substrate in structure, the kind of the inhibitor drugs can compete with the binding of substrates for the enzyme. The drug efficacy is produced as long as the drug is combined with the enzyme (producing E·EID). When the concentration of EID diminishes because of metabolism, the concentration of complex E·EID diminishes and the drug efficacy decreases. Administration of the drug several times a day is necessary to maintain the drug efficacy. In the section, the mechanism-based enzyme

inactivator is adopted in drug reception process based on the Michaelis Menten enzymatic kinetics, which is formulated as Eq.(13).

$$E + EID \underset{k_{off}}{\overset{k_{on}}{\rightleftharpoons}} E \cdot EID \xrightarrow{k_2} E \cdot EID' \tag{13}$$

where k_{on}, k_{off} are the reaction rate constant, k_2 is turnover number in reaction, E·EID' an unreactive compound with the properties of specificity and low toxicity, EID the enzyme inhibitor drugs. The update of the concentration [EID] follows Fick's second law

$$\frac{\partial [EID]}{\partial t} = D_D \nabla^2 [EID] \tag{14}$$

where D_D is the diffusion coefficient of the enzyme inhibitor drug, ∇^2 Laplacian for the dimension considered. It is assumed that each tumor cell corresponds to an enzyme (e.g., tyrosine kinase) and it die when the enzyme is inactivated. If the total amount of enzyme E is constant, increasing drug release rate decreases the efficiency while results in higher reaction rate [28]. It is obvious that constant drug release rate decreases the efficiency while results in lower reaction rate when the total amount E decreases (i.e., the number of tumor cells decreases). It is necessary to adjust drug release rate in order to maintain efficiency. It is assumed that the molecular concentration of tumor biomarker is proportional to the number of tumor cells. The adjustable drug release rate based on the concentration of tumor biomarker is formulated as Eq.(15)

$$Q_D = \frac{L\, J(i,j)}{K + J(i,j)} \tag{15}$$

where K, L are constants associated with the release rate, $J(i,j)$ the concentration of tumor biomarker.

5 Simulations and Results

In the section, we in order to establish our simulations. First, we establish the simulation environment and configure the parameters in simulation. The next involves simulation results and analysis.

5.1 Simulation Setup

In this subsection, a three-dimensional space called simulation space is established with volume of $x \times y \times z = 100$ patches $\times$ 100 patches $\times$ 100 patches, where patch is length unit in simulation. The origin of the simulation space is at $O(x, y, z) = O(0, 0, 0)$ and the coordinate range is $(-50 \leq x \leq 50, -50 \leq y \leq 50, -50 \leq z \leq -50)$. N nanorobots emerge randomly from $S(-40, -40, -40)$ in the simulation space with random motion directions. It is assumed that

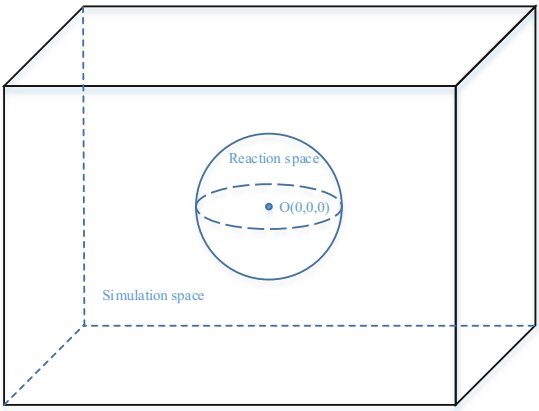

Fig. 1. Simulation and reaction space.

Table 2. Simulation parameters.

Symbol	Description	Value
N	Number of nanorobots	123
R	Radius of reaction space	3 patch
s	Nanorobot motion speed	0.2 patch/tick
Q_A	Release rate of AI	5 molecules/tick
D_A	Diffusion coefficient of AI	1 patch^2/tick
T_{AIl}	Quorum sensing threshold (Low threshold of AI)	15 molecules/patch^3
T_{AIh}	High threshold of AI	60 molecules/patch^3
K	Release rate constant	200
L	Release rate constant	500
D_D	Diffusion coefficient of drug	1 patch^2/tick
n_T	Number of tumor cells	1500
n_E	Number of enzymes	1500
k_2	Turnover number	0.02/tick
k_{on}	Reaction rate constant	0.2/tick
k_{off}	Reaction rate constant	0.03/tick

tumor cells are distributed randomly in a three-dimensional space named reaction space. The reaction space is a sphere of radius $R = 3$ patches and its center locates at $O(0, 0, 0)$ (see Fig. 1). The diffusion of tumor biomarker follows Fick's second law and Eq.(7), that is, the concentration of tumor biomarker is inversely proportional to the distance from the tumor target site.

Nanorobots simulate bacterial chemotaxis to approach reaction space with speed $s = 0.2$ patches/tick, where tick is time unit in simulation. Nanorobots release AI molecules as long as entering into reaction space. When AI molecules

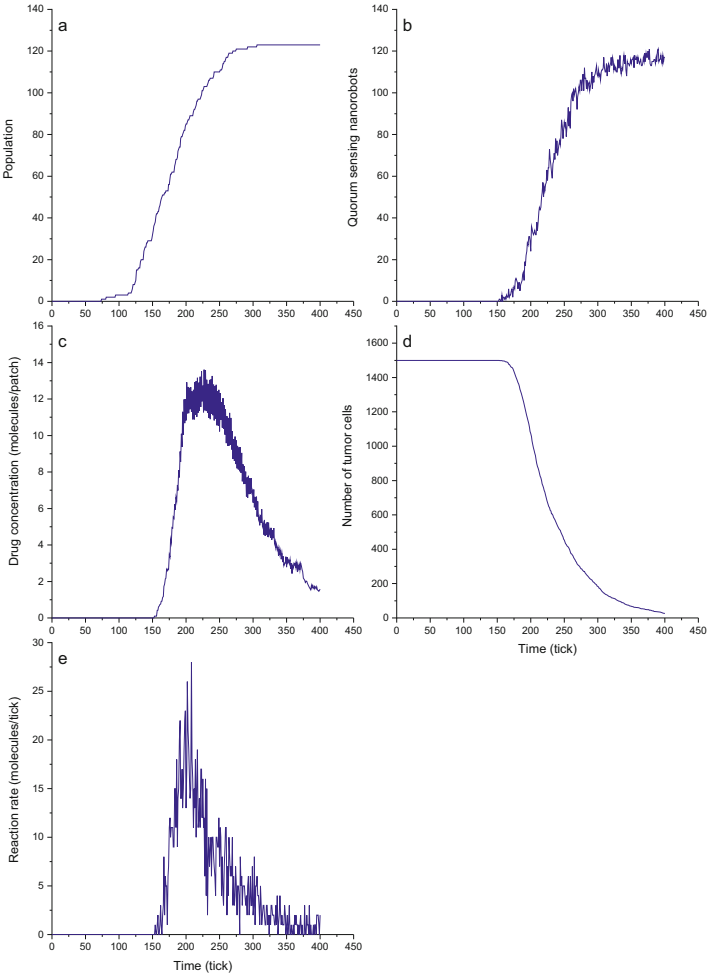

Fig. 2. Variation in simulation of drug delivery system.

exit simulation space, they are removed from the simulation, in order to limit the computational burden of the simulation. Nanorobots report the number of molecules found within the patch which the nanorobot locates at in each time step (tick). It is considered that molecular concentration is constant over such volume of V =1 patch^3 due to small dimensions, and nanorobots are arranged in a perfect tridimensional sphere grid with radius $R = 3$ patches and center coordinate $O(0, 0, 0)$, and the distance between adjacent nanorobots is $l = 1$ patch. Hence, the molecular concentration sensed by a nanorobot at a patch of volume V located at a distance r from the center of reaction space can be calculated by Eq.(11). The threshold of quorum sensing T_{AIl} of nanorobots can be obtained from Eq.(12). The drug reception in reaction space follows Michaelis Menten

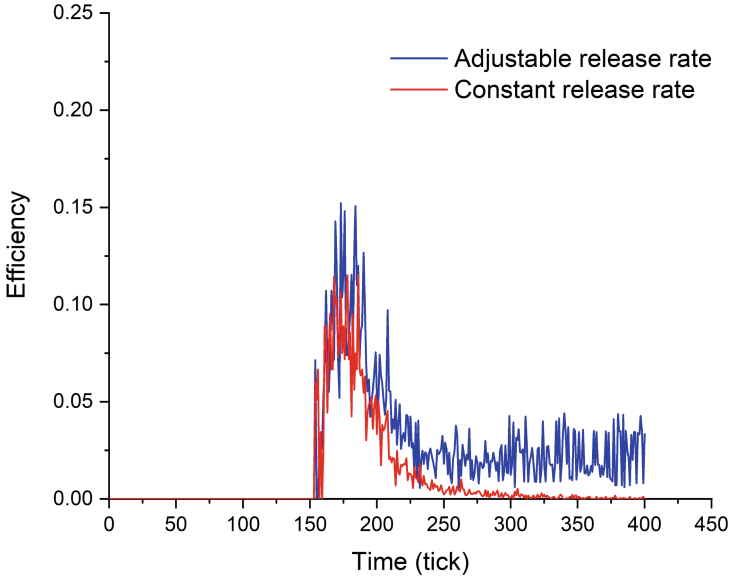

Fig. 3. Efficiency of drug utilization: (a) the blue curve represents the adjustable release rate based on the concentration variation of tumor biomarker molecules, (b) the red curve represents constant release rate. (Color figure online)

enzymatic kinetics formulated as Eq.(13). The main simulation parameters and physical descriptions are shown in Table 2.

5.2 Simulation Results and Analysis

Figure 2(a) shows the change in the number of nanorobots arriving in reaction space, and Fig. 2(b) shows the change in the number of quorum sensing nanorobots as time increases in simulation. As shown in Fig. 2(b), the first nanorobot reaches quorum at time $t = 153$ ticks, all nanorobots reach quorum at about $t = 400$ ticks, and the majority of nanorobots reach quorum in the time of $t = 200 \sim 275$ ticks. Obviously there is a delay from the first nanorobot to all nanorobots reaching quorum. This is because the concentration of AI molecules decreases as the distance increases from the center of reaction space, that is, when the nanorobots close to the center reach quorum, those close to the edge do not yet reach quorum due to the low AI concentration below the threshold T_{AIl}. Figure 2(c) shows the variation of drug concentration as time increases. The drug concentration detected by a nanorobot is the number of drug molecules in a $patch^2$ where the nanorobot locates. From Figs. 2(a), (b) and (c), we observe that nanorobots rather release drugs until they reach quorum than as soon as they reach the reaction space. Figure 2(d) shows the change in the number of tumor cells as time increases. If release rate is constant, decreasing number of tumor cells decreases the reaction rate while results in lower efficiency according to enzymatic reaction kinetics formulated as Eq. (13). Figure 2(e) shows the

variation of reaction rate as time increases in simulation. The reaction rate measured is the number of unreactive compound E·EID′ produced by reactions of drugs and enzymes per tick.

Figure 3 shows the variation of efficiency in simulation. The efficiency is the reaction rate divided by the sum of release rates of nanorobots reaching quorum. As shown in Fig. 3, the blue line represents the variation of efficiency under the adjustable release rate based on the concentration of tumor biomarker, while the red represents the variation under the constant release rate $Q_D = 30$ molecules/(2 ticks). Obviously the adjustable release rate enhances the efficiency compared with that constant release rate, thus saving drug and preventing drug overuse.

6 Conclusions

In this paper, we proposed a nanorobot-based system comprising of nanorobot behavior planning (NBP) algorithm, drug reception model and adjusting method of release rate. In NBP algorithm, each nanorobot is considered as a bacterium with specified chemotaxis and quorum sensing behavior. After reaching the tumor location by simulating bacterial chemotaxis, nanorobots determine the timing of drug release relying on quorum sensing to release drugs. The quorum threshold is calculated that ensure the quorum sensing of all of the nanorobots in reaction space. Under the drug reception based on enzymatic reaction kinetics, an adjustable rate of drug release is designed based on the concentration of tumor biomarker. Finally, we established the simulation environment reflecting the property of concentration, diffusion-rate of AI and drug molecles. The simulation results show that the nanorobot-based system not only enables nanorobots to reach target site and release drug molecules after they reach quorum, but also enhances the efficiency of drug utilization.

References

1. Hoffman, A.S.: The origins and evolution of “controlled” drug delivery systems. J. Control. Release **132**(3), 153–163 (2008)
2. Bae, Y.H., Park, K.: Targeted drug delivery to tumors: myths, reality and possibility. J. Control. Release **153**(3), 198–205 (2011)
3. Davis, F.F.: The origin of PEGnology. Adv. Drug Deliv. Rev. **54**(4), 457–458 (2002)
4. Maeda, H., Ueda, M., Morinaga, T., Matsumotog, T.: Conjugation of poly(styrene-co-maleic acid) derivatives to the antitumor protein neocarzinostatin: pronounced improvements in pharmacological properties. J. Med. Chem. **28**(4), 455–461 (1985)
5. Matsumura, Y., Maeda, H.: A new concept for macromolecular therapeutics in cancer chemotherapy:mechanism of tumoritropic accumulation of proteins and the antitumor agent smancs. Can. Res. **46**, 6387–6392 (1986)
6. Maeda, H., Matsumura, Y.: EPR effect based drug design and clinical outlook for enhanced cancer chemotherapy. Adv. Drug Delivery Rev. **63**(3), 129–130 (2011)
7. Harris, J.M., Martin, N.E., Modi, M.: Pegylation -a novel process for modifying pharmacokinetics. Clin. Pharmacokinet. **40**, 539–551 (2001)

8. Kizelsztein, P., Ovadia, H., Garbuzenko, O., Sigal, A.: Pegylated nanoliposomes remote-loaded with the antioxidant tempamine ameliorate experimental autoimmune encephalomyelitis. J. Neuroimmunol. **213**(1–2), 20–25 (2009)
9. Taurin, S., Nehoff, H., Greish, K.: Anticancer nanomedicine and tumor vascular permeability; where is the missing link? J. Contr. Release Off. J. Controll. Release Society **164**(3), 265–275 (2012)
10. Beduneau, A., Saulnier, P., Hindre, F., Clavreul, A., Leroux, J.C., Benoit, J.P.: Design of targeted lipid nanocapsules by conjugation of whole antibodies and antibody Fab' fragments. Biomaterials **28**(33), 4978–4990 (2007)
11. Deckert, P.M.: Current constructs and targets in clinical development for antibody-based cancer therapy. Curr. Drug Targets **10**(2), 158–175 (2009)
12. Zoabi, N., et al.: The evolution of tumor-targeted drug delivery: from the EPR effect to Nanoswimmers. Isr. J. Chem. **53**, 719–727 (2013)
13. Baban, C.K., Cronin, M., O'Hanlon, D., O'Sullivan, G.C., Tangney, M.: Bacteria as vectors for gene therapy of cancer. Bioengineered Bugs **1**(6), 385–394 (2010)
14. Akin, D., Sturgis, J., Ragheb, K., Sherman, D., Burkholder, K.: Bacteria-mediated delivery of nanoparticles and cargo into cells. Nat. Nanotechnol. **2**(7), 441–449 (2007)
15. Liu, Y., et al.: Bacteria-mediated in vivo delivery of quantum dots into solid tumor. Biochem. Biophys. Res. Commun. **425**(4), 769–774 (2012)
16. Cavalcanti, A., Hogg, T., Shirinzadeh, B., Liaw, H.C.: Nanorobot communication techniques: a comprehensive tutorial. In: 9th International Conference on Control, Automation, Robotics and Vision, pp. 1–6. Singapore (2006)
17. Tredan, O., Galmarini, C.M., Patel, K., Tannock, I.F.: Drug resistance and the solid tumor microenvironment. J. Natl Cancer Inst. **99**(19), 1441–1454 (2007)
18. Tannock, I., Lee, C., Tunggal, J.: Limited penetration of anticancer drugs through tumor tissue a potential cause of resistance of solid tumors to chemotherapy. Clin. Cancer **8**, 878–884 (2002)
19. Bassler, B.L., Losick, R.: Bacterially speaking. Cell **125**(2), 237–246 (2006)
20. Cobo, L.C., Akyildiz, I.F.: Bacteria-based communication in nanonetworks. Nano Commun. Netw. **1**(4), 244–256 (2010)
21. Akyildiz, I.F., Brunetti, F., Blazquez, C.: Nanonetworks: a new communication paradigm. Comput. Netw. **52**(12), 2260–2279 (2008)
22. Miller, M.B., Bassler, B.L.: Quorum sensing in bacteria. Annu. Rev. Microbiol. **55**(1), 165–199 (2001)
23. Philibert, J.: One and a half century of diffusion: Fick, Einstein, before and beyond. Diff. Fundamentals **4**(6), 1–19 (2006)
24. Bossert, W.H., Wilson, E.O.: The analysis of olfactory communication among animals. J. Theor. Biol. **5**(3), 443–469 (1963)
25. Shahmohammadian, H., Messier, G.G., Magierowski, S.: Optimum receiver for molecule shift keying modulation in diffusion-based molecular communication channels. Nano Commun. Netw. **3**(3), 183–195 (2012)
26. Abadal, S., Llatser, I., Alarcón, E., Cabellos-Aparicio, A.: Cooperative signal amplification for molecular communication in nanonetworks. Wirel. Netw. **20**(6), 1611–1626 (2014)
27. Silverman, R.B.: Mechanism-based enzyme inactivators. In: Purich DL Contemporary enzyme kinetics and mechanism. Academic Press, Burlington (2009)
28. Zhao, Q., Li, M., Luo, J.: Relationship among reaction rate, release rate and efficiency of nanomachine-based targeted drug delivery. Technol. Health Care **25**(6), 1119–1130 (2017)